INFLUENCE OF COOLING RATE ON THE PROPERTIES AND CHARACTERIZATIONS OF ALUMINIUM-BASED CAST PARTICULATE *IN-SITU* COMPOSITE

Abdulhaqq A. Hamid Al-dabbagh

Mechanical Eng. Dept. - College of Engineering - University of Mosul
E-Mail: abdulhaqqhamid@yahoo.com

Abstract

The current work focused on the influence of cooling rate on the microstructure, mechanical and tribological properties of cast *in-situ* composite. It was observed that the size of intermetallic phase $Mn(Al_{1-x}Fe_x)_6$ and the dendrite arm spacing (DAS) increases considerably with decreasing cooling rate of the cast ingot. Microstructural examination of these different cast *in-situ* composites shows that there is no significant difference in the size of the *in-situ* formed alumina particle. Superior mechanical properties, as indicated by ultimate tensile stress, yield stress, percentage elongation and hardness, are obtained when the *in-situ* composites are processed by cooling the cast ingot in water, resulting in refined microstructure. Higher hardness due to refined microstructure and superior mechanical properties result in decreased wear rate in cast *in-situ* composites cooled in water after casting, compared to the wear rates observed in cast ingots cooled either in air or inside furnace. Cast *in-situ* composite cooled in water after casting, shows higher coefficient of friction compared to those cooled in air or inside furnace.

Keywords Cast *In-situ* Composite, Al-Al_2O_3; Cooling Rate; Microstructure; Mechanical Properties; Dry Sliding; Wear; Friction.

تأثير معدل التبريد على خواص ومواصفات الألمنيوم المتراكب من الداخل بالجسيمات الدقيقة

د. عبدالحق عبدالقادر حامد الدباغ

قسم الهندسة الميكانيكية ـ كلية الهندسة ـ جامعة الموصل ـ موصل/العراق

الخلاصة

في هذا البحث الحالي ركزت الدراسة على تأثير معدل التبريد على التركيب ألمجهري, والخواص الميكانيكية وخواص الاحتكاك والبرئ للمادة المتراكبة. حيث وجد أن حجم الطور $Mn(Al_{1-x}Fe_x)_6$ والمسافة (DAS) يزدادان مع تناقص معدل التبريد للمسبوك. وكما أن الاختبار ألمجهري لهذه المسبوكات المختلفة بين بأنة لايوجد اختلاف في حجم دقائق الالومينا المتولدة من الداخل. وكذلك وجد أن معدل التبريد له تأثير كبير ومباشر على تركيبة وخواص المادة المتراكبة, حيث أن الخواص الميكانيكية والمتمثلة بالجهد الاقصى للفشل, وجهد الخضوع, والمطاطية, والصلادة تكون اكبر في المواد التي كان تبريدها بالماء. وبشكل عام, فالتركيبة المجهرية الصغيرة والنقية والخواص الميكانيكية العالية والتي سببها معدل التبريد العالي أدى بالتالي إلى انخفاض معدل البرئ بشكل كبير مقارنة مع المواد المتراكبة والتي معدل تبريدها اقل. وان معامل الاحتكاك أعلى في المادة المتراكبة التي معدل تبريدها عالي مقارنة مع المواد المتراكبة والتي معدل تبريدها اقل كما هو الحال في التبريد في الهواء أو في داخل الفرن.

Received 1 Oct. 2008 Accepted 12 Mar. 2009

1. Introduction

The growing sophistication of structural and tribological applications in both military and civilian segments are compelling materials scientists, engineers and researchers worldwide to innovate novel materials that reduce weight, maximize fuel efficiency and satisfy other requirements in engineering applications. Also, the rising oil prices compelled the automobile industries to look for better fuel economy and lighter vehicles which has opened the door to usage of lightweight metal matrix composites in a sector known for high volume use of materials [1]. There is no denial of the fact that weight saving in a vehicle reduces the requirement of the engine capacity for the same performance and thereby, results in a cheaper car. Therefore, the agenda of weight saving in a car will remain alive reinforced at times by step escalation of fuel price. Development of cast metal matrix composites, the cheapest material in composites category, is primarily motivated by the interest of automobile industries which can afford its price range. It is perceived that composite materials are going to make a big difference in automobiles with progress of time [1, 2].

The particular attributes of aluminium based composites are a combination of high specific stiffness, high creep resistance, good fatigue properties and the potential for relatively low cost [2]. It is possible to tailor the mechanical and thermal properties of these materials to meet the requirements of a specific application. To do this, there are a number of variables, which need to be considered; these include the type and level of reinforcement, the choice of the matrix alloy, the composite processing route and the processing parameters. All these factors are interrelated and should not be considered in isolation when developing a new material.

As noted recently, *in-situ* generation of reinforcements in a metal matrix offers a route to achieve a wide range of attractive material properties that cannot be obtained either in *ex-situ* composites or conventional alloys. The superior material properties in *in-situ* composites are the direct result of relatively more uniform distribution of *in-situ* generated reinforcing particles inside the matrix alloy, good wettability between the virgin surface of *in-situ* generated particles and the molten matrix alloy, thermal equilibrium between the particles and the matrix alloy and better bonding between the particles and the matrix non-interfered by contamination [3-7]. However, the production of *in-situ* PMMCs by solidification processing is attractive due to their low cost, contributed also by the value added through release of alloying elements from relatively cheaper oxides, flexibility in operation and potential to integrate with standard foundry practice. In the area of cast *in-situ* Al-Al_2O_3 composites, two different routes are used for generating oxide particles- (i) direct oxidation of molten aluminum alloy [8] and (ii) substitution reaction between molten aluminum and metal oxide, such as TiO_2 [9,10], MnO_2 [11], B_2O_3 [12], MoO_3 [13,14]. In the latter method, cast *in-situ* aluminium alloy-Al_2O_3 composites are obtained as the resulting product when the externally added metal oxide gets reduced by molten aluminium to generate alumina particles and release useful alloying elements in the remaining molten aluminium.

In previous work it has been shown that the generation of *in-situ* TiB_2 [15] into aluminium alloys, improves the wear resistance significantly. Also, the wear resistance of *in-situ* Al-Ti_3Al composite is superior to that observed in Al-Ti base alloys having the same titanium content and even to that of SiC whisker reinforced aluminium based *ex-situ* composite having the same volume fraction of SiC reinforcement [16]. Furthermore, the excellent mechanical properties in aluminium based *in-situ* composites qualify them to be candidate materials for many engineering applications. Therefore, the present work is intended to investigate the material characteristics and tribological behaviour of cast *in-situ* Al(Mg,Mn)-Al_2O_3(MnO_2) composites synthesized by dispersing MnO_2 particles into molten aluminium. Manganese released to the alloy by reduction of MnO_2 particles by molten aluminium, may play a limited role as a grain

refiner and as an iron corrector [17]. Therefore, the interesting feature of this system is expected to arise from matrix strengthening by *in-situ* reinforcing particles of alumina as well as from alloying of molten aluminium by manganese. The studies undertaken here are expected to lead to an understanding of the overall materials characteristics and tribological behaviour due to matrix strengthening by alloying of manganese and also by reinforcing hard particles.

2. Experimental Procedure

In the present study, cast aluminium alloy-based composites containing *in-situ* generated alumina particles, have been synthesized by stirring MnO_2 particles into molten aluminium alloy using pitch blade stirrer, followed by addition of small amounts of surface active element of magnesium (Mg) and the resulting slurry is cast into a permanent steel mould by bottom pouring, according to a similar procedure detailed elsewhere [11]. The photographic picture of the experimental set up used in the current investigation is shown in Fig.1. The cast *in-situ* composite ingots were cooled after casting, at different rates by cooling in water bath (about 450 ^{o}C/min) or in air (about 75 ^{o}C/min) or in a furnace (about 8 ^{o}C/min). The rate of cooling of cast ingot was estimated with the help of a chromel-alumel thermocouple placed at the centre of the cast ingot.

The tensile tests were carried out at ambient temperature for the cast *in-situ* composites. The specimens were machined from each cast ingot. The shape (bone type) and dimension of the tensile specimens are conforming to ASTM specification. At least three tensile specimens of 5.0 mm gauge diameter and 25 mm gauge length, machined out from each segment of each cast *in-situ* composite, were tested under uniaxial tension in a Hounsfield, Monsanto, H25KS/05, Surrey, England, tensile testing machine at a strain rate of 6.6×10^{-4} s^{-1} and the average of ultimate tensile strength, yield strength and percentage elongation is reported as the tensile property of the material. After fracture of the specimens, the fracture surfaces were examined under scanning electron microscope and characteristic features of all the fracture surfaces were photographed. The methods used for determination of chemical composition of the matrix alloy, particle content, porosity and mechanical properties of cast *in-situ* composites are similar to that given in details in Reference [11].

Dry sliding wear tests were carried out by sliding a cylindrical pin, with a flat polished end against a counterface of hardened steel disc under ambient condition (relative humidity is about 50% and ambient temperature is about 25 ^{o}C) using a pin-on-disc machine, model TR-20E manufactured by DUCOM, Bangalore, India. The photographic view of a pin-on-disc machine used in the current investigation is shown in Fig.2. The test pin has a diameter of 6 mm and length of 30 mm. The counterface disc is made of EN-32 steel hardened to 62-65 HRC. Different loads of 9.8, 19.6, 29.4, 34.3 and 39.2 N were applied on the pin normal to the sliding contact surface during wear test of each cast *in-situ* composite. The track radius was kept constant at 50 mm and the rotating speed of the disc was maintained at 200 rpm, corresponding to a linear sliding speed of 1.05 m/s. The wear tests are carried out for a total sliding distance of about 3142 m. The cumulative weight loss was measured by interrupting a wear test at regular intervals of five minutes. An electronic balance (Mettler AJ 100) having least count of 0.01 mg, was used to measure the weight loss. The cumulative volume loss after a given sliding distance was determined by dividing the cumulative weight loss by the density of the test pin. The densities of the cast *in-situ* composites were determined by using a pycnometer. The frictional force is monitored continuously during the wear tests, to determine the coefficient of friction. In order to test reproducibility, the wear tests were replicated thrice and the mean results of cumulative

volume loss with sliding distance were used for further calculations of wear rates and wear coefficients.

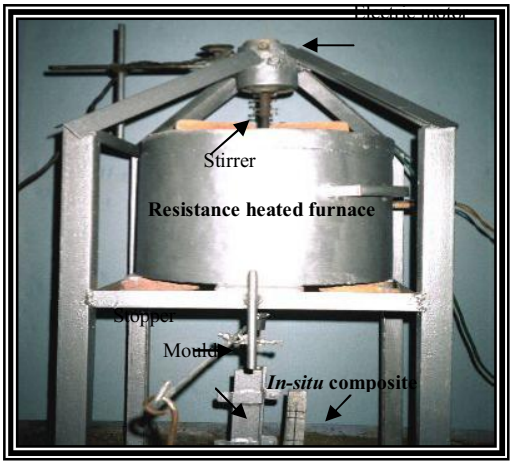

Figure1. Photographic view showing experimental set-up for stir casting used for solidification processing of different cast *in-situ* composites.

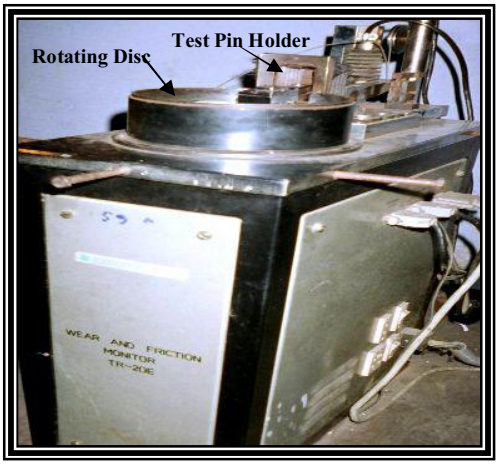

Figure 2. Photographic view showing a pin-on-disc machine, model TR-20E, used for wear and friction tests of different cast *in-situ* composites.

3. Results and Discussion

Ingots of cast *in-situ* composites of nominal composition of Al(5%Mg)-3%MnO_2, synthesized at 730 ^oC for three minutes of processing have been cooled after casting, at different rates by cooling in water bath or in the air or in the furnace. Figure 3 shows typical unetched microstructures of cast *in-situ* Al(Mg,Mn)-Al_2O_3(MnO_2) composites cooled after casting at different cooling rates and it consists of intermetallic phase Mn $(Al_{1-x}Fe_x)_6$ forming due to release of manganese to the matrix alloy beyond the limit of solid solubility, by reduction of manganese dioxide by molten aluminium. The microstructures reported in the present study relate to those observed in the middle height segment of the cast ingot unless stated otherwise. Some dark areas of porosity are also visible. It is further observed that porosity, primarily originating from the gases dissolved into melt during processing, is more or less uniformly distributed in the matrix alloy of the cast *in-situ* composites. However, there is sometimes large porosity around cluster of particles, particularly at the top of the cast ingot of *in-situ* composite. Iron in the intermetallic phase has also been contributed by iron pick-up from alumina coated steel stirrer. The estimated volume fraction of the intermetallic phase $Mn(Al_{1-x}Fe_x)_6$ in the microstructures of these cast *in-situ* composites are reported in Table 1. It is observed that as the cooling rate decreases, the extent of reaction of MnO_2 particles with molten aluminium alloy increases as evident from the amount of intermetallic phase $Mn(Al_{1-x}\ Fe_x)_6$ in the matrix of cast *in-situ* composite as reported in Table 1. It is also observed that the size of intermetallic phase $Mn(Al_{1-x}Fe_x)_6$ increases with decreasing cooling rate as shown in Fig. 3.

The etched microstructures of cast *in-situ* composites cooled at different cooling rates after casting are shown in Fig. 4. It is observed that as the cooling rate decreases, the dendrite arm spacing (DAS) increases considerably as evident from the microstructure in Fig. 4. A comparison between porosity and particle contents for cast *in-situ* composite ingot cooled at different cooling rates after casting are shown in Figs. 5 and 6 respectively. It is observed that there is no

significant difference observed either in respect of porosity or particle contents in ingots cooled at different cooling rates after casting as shown in Figs. 5 and 6.

Table 1. Average volume fractions of the intermetallic phase in the microstructure of cast *in-situ* composites cooled after casting at different cooling rates.

Cooling rate (^{o}C/min)	Average volume fraction (vol%)
Water cooling (≈450)	3.53±0.79
Air cooling (≈75)	3.61±0.63
Furnace cooling (≈8)	4.53±0.68

The amount of reacted MnO_2 particles in the cast *in-situ* composite of nominal composition of Al(5%Mg)-3%MnO_2, synthesized at processing temperature of 730 ^{o}C for three minutes of processing, followed by cooling after casting at different rates has been estimated as shown in Fig. 7. The MnO_2 particles reacted are more in the cast *in-situ* composite cooled in a furnace after casting.

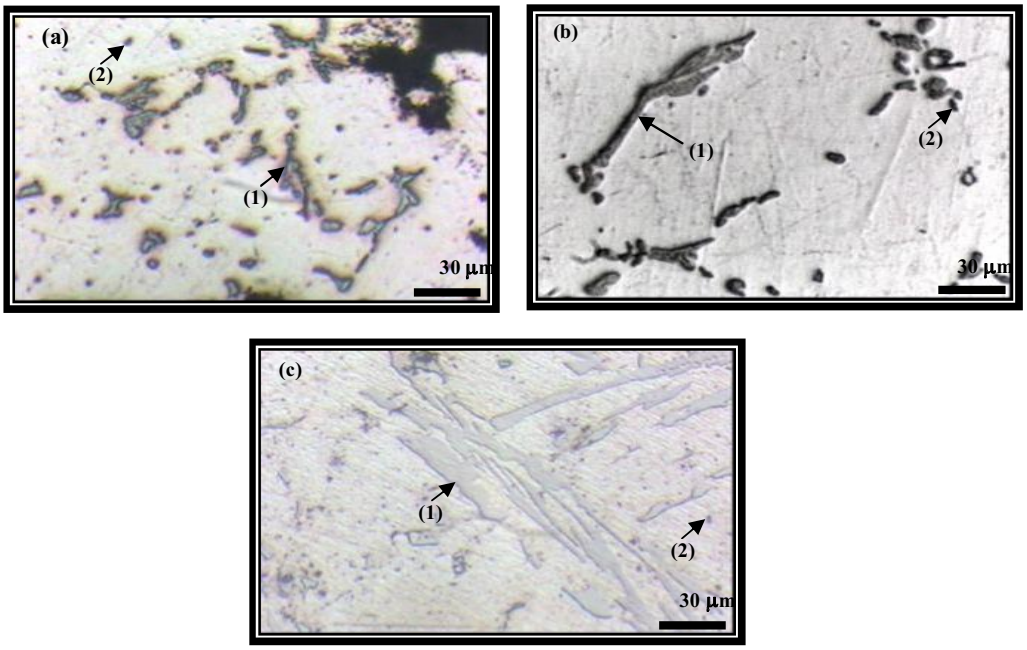

Figure 3. Unetched optical microstructures of cast *in-situ* composites of nominal composition of Al(5%Mg)-3%MnO_2, synthesized at processing temperature of 730 ^{o}C for three minutes of processing, followed by different methods of cooling; (a) water cooling, (b) air cooling and (c) furnace cooling; the intermetallic phase $Mn(Al_{1-x}\ Fe_x)_6$ marked by (1) and the reinforcing particles marked by (2).

Gases are absorbed to different extents in molten metals and alloys. Since, the processing of cast *in-situ* composite involves mixing of particles with molten alloy which has been carried by stirring in air, there is considerable dissolution of environmental gases like O_2, N_2 and most significantly H_2, contributed by moist air. No degassing practice has been followed here. The dissolved gases will evolve with cooling due to lowering of limit of solubility, nucleating bubbles heterogeneously on solid particles and on solidification there is dramatic reduction in the solubility of gases. These bubbles are primarily responsible for porosities in cast composite.

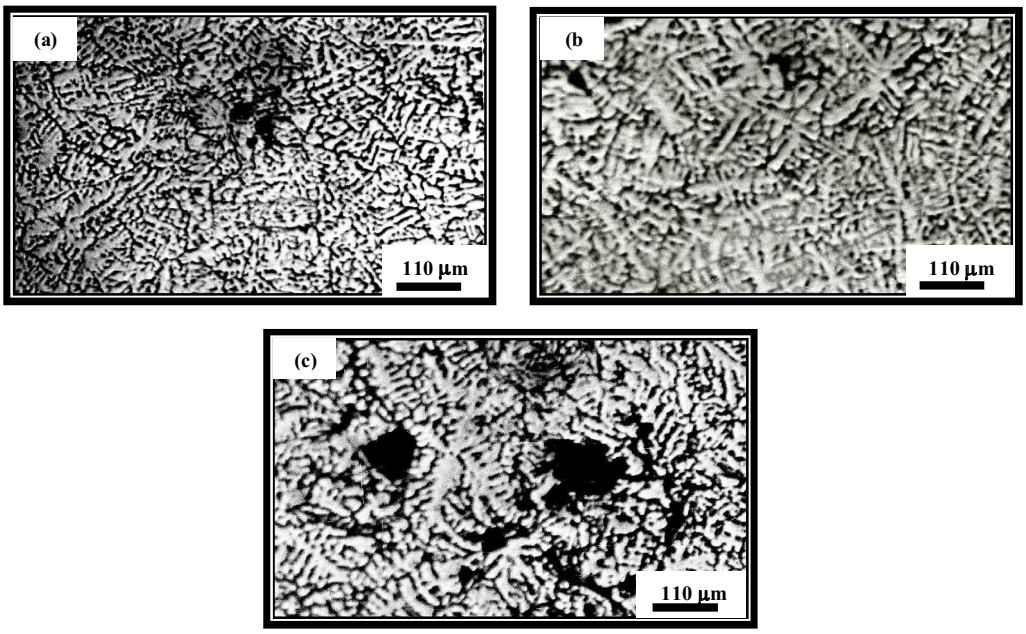

Figure 4. Etched optical microstructures of cast *in-situ* composites of nominal composition of Al(5%Mg)-3%MnO_2, synthesized at processing temperature of 730 ^oC for three minutes of processing, followed by different methods of cooling; (a) water cooling (about 450 ^oC/min), (b) air cooling (about 75 ^oC/min) and (c) furnace cooling (about 8 ^oC/min).

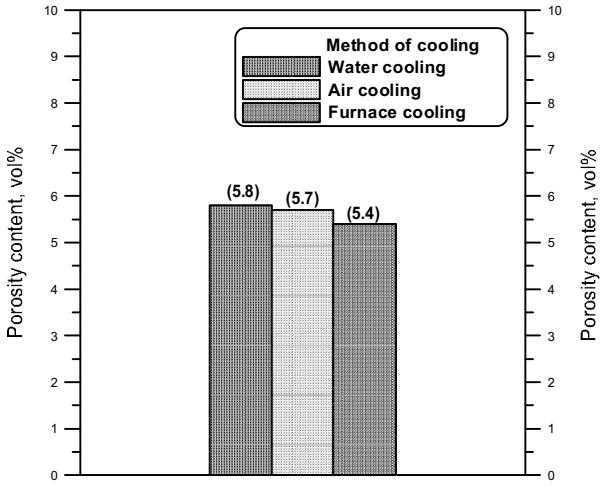

Figure 5. Comparison between average porosity content for cast *in-situ* composite ingot of nominal composition of Al(5%Mg)-3%MnO_2, cooled after casting at different cooling rates.

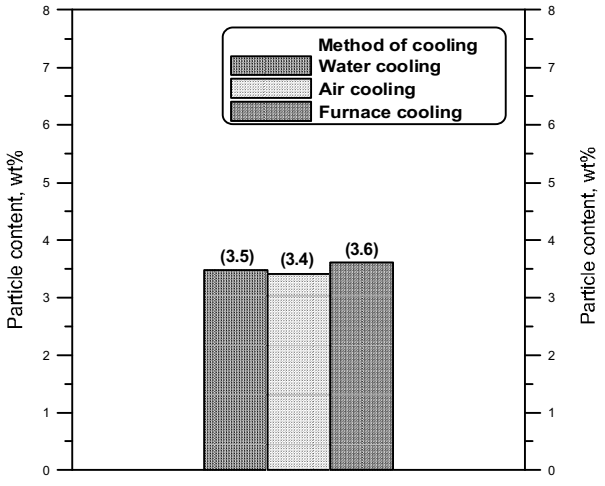

Figure 6. Comparison between average particle content for cast *in-situ* composite ingot of nominal composition of Al(5%Mg)-3%MnO_2, cooled after casting at different cooling rates.

The effect of different cooling rates on the Brinell hardness of cast *in-situ* composites of nominal composition of Al(5%Mg)-3%MnO_2, synthesized at processing temperature of 730 ^oC for three minutes of processing is shown in Fig. 8. The average Brinell hardness of cast *in-situ* composites cooled after casting by immersion in water bath is considerably greater than that for cast *in-situ* composite cooled either in air or inside the furnace as demonstrated in Fig. 8.

Microstructural examination of these ingots of cast *in-situ* composites cooled at different cooling rates showed that the intermetallic phase $Mn(Al_{1-x}Fe_x)_6$ coarsened gradually and its volume fraction increases with decreasing cooling rate (see Fig. 3). In addition, it is seen that slow cooling generated a coarser dendrite size as demonstrated in Fig. 4. As the cooling rate decreases, the secondary dendrite arm spacing (DAS) increases. Therefore, refined intermetallic phase and refined dendrite structure are both responsible for a higher level of hardness in cast *in-situ* composite cooled relatively faster in water after casting.

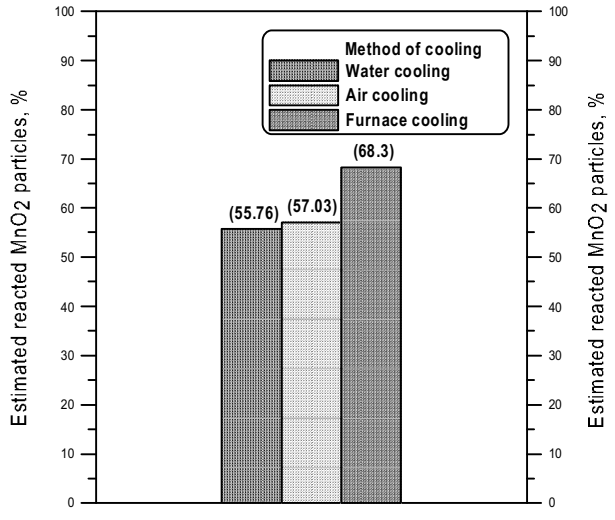

Figure 7. Comparison between estimated reacted MnO_2 particles for cast *in-situ* composite ingot of nominal composition of Al(5%Mg)-3%MnO_2, cooled after casting at different cooling rates.

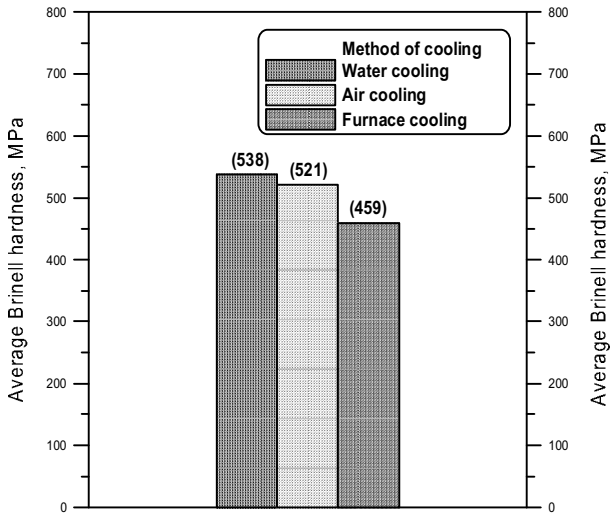

Figure 8. Comparison between average Brinell hardness for cast *in-situ* composite of nominal composition of Al(5%Mg)-3%MnO_2, synthesized at processing temperature of 730 ^oC for a given processing time of three minutes, cooled after casting by different methods of cooling.

Figure 9 shows the experimental load-extension curves of cast *in-situ* Al(Mg,Mn)-$Al_2O_3(MnO_2)$ composites cooled after casting at different cooling rates. The average tensile properties of cast *in-situ* composites cooled after casting by immersion in water bath is considerably greater than that observed for cast *in-situ* composite cooled either in air or inside furnace as demonstrated in Figs. 9 and 10. Refined intermetallic phase and dendrite structure are both responsible for a higher level of strength in cast *in-situ* composite cooled in water after casting.

The tensile fractured surfaces of the specimens subjected to tensile test have been studied under optical and scanning electron microscopy (SEM) for the different cast *in-situ* composites. Figures 11(a) and (b) shows the typical macrographs as observed under optical microscope of the fractured surface of specimen after tensile test of cast *in-situ* composite showing better mechanical properties and containing 2.9 wt% reinforcing particles and 2.4 vol% porosity. It appears that the crack has propagated through an angle between 40^o–50^o from the loading axis, as shown in Fig. 11(a), resulting in an ultimate tensile stress of 239 MPa and percentage elongation of 21.3%.

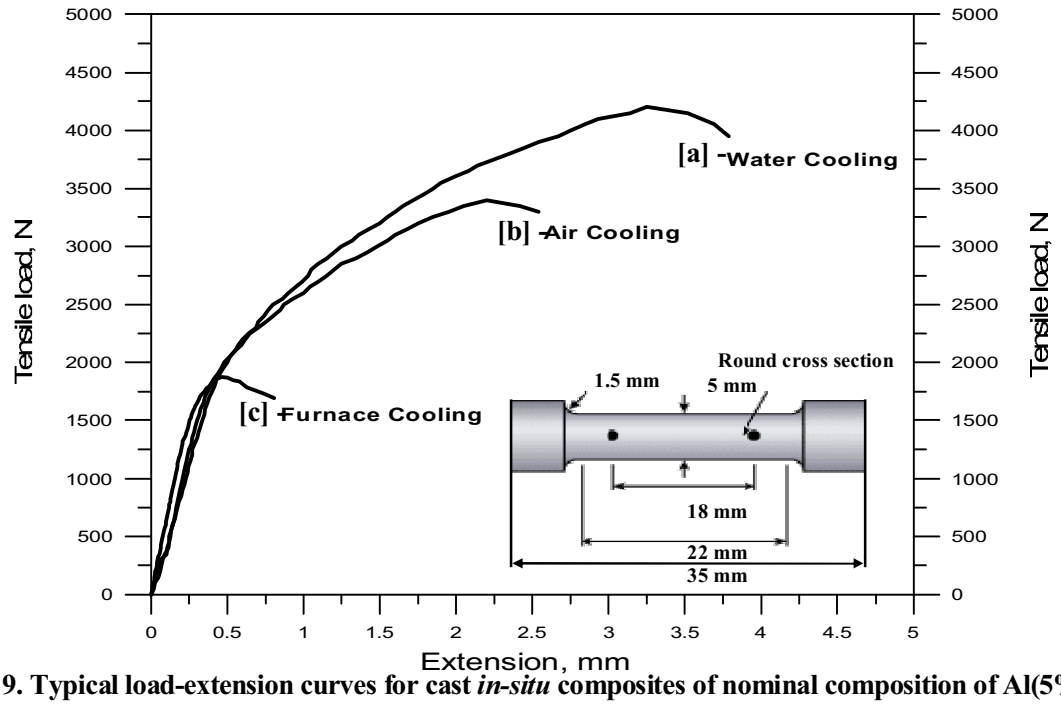

Figure 9. Typical load-extension curves for cast *in-situ* composites of nominal composition of Al(5%Mg)-3%MnO_2, synthesized at processing temperature of 730 ^{o}C for three minutes of processing, followed by different methods of cooling; (a) water cooling, (b) air cooling and (c) furnace cooling.

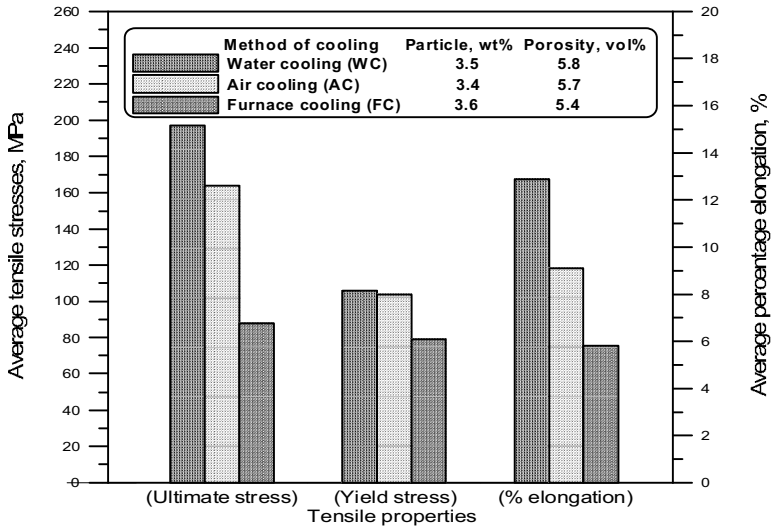

Figure 10. Comparison between average tensile properties for cast *in-situ* composite resulting from nominal composition of Al(5%Mg)-3%MnO_2, synthesized at processing temperature of 730 ^{o}C for three minutes of processing, cooled after casting at different cooling rates.

Figure 12 shows the typical fractured surfaces for the different cast *in-situ* composites as observed under scanning electron microscopy. The fractured surface of the specimen shown in Figs. 12(a), (b) and (c) belongs to a cast *in-situ* composite cooled after casting in (a) water, (b) air and (c) inside furnace respectively. In case of cast *in-situ* composite cooled after casting in water, the tensile fracture surface shows the presence of both sheared regions and dimples as revealed in Fig. 12(a), resulting in a percent elongation of 21.3%. The fractured surface of a cast *in-situ*

composite cooled after casting in air is similar to that observed in cast *in-situ* composite cooled after casting in water as shown in Fig. 12(b). But, in case of cast *in-situ* composite cooled after casting in furnace, the fractured surface shows the presence of porosity around particles, leading to large voids and the ductile fracture of the matrix between the voids, as evidence from dimples as shown in Fig. 12(c). There are also areas of sheared fracture around the voids resulting in an overall elongation of only about 3.42 percent.

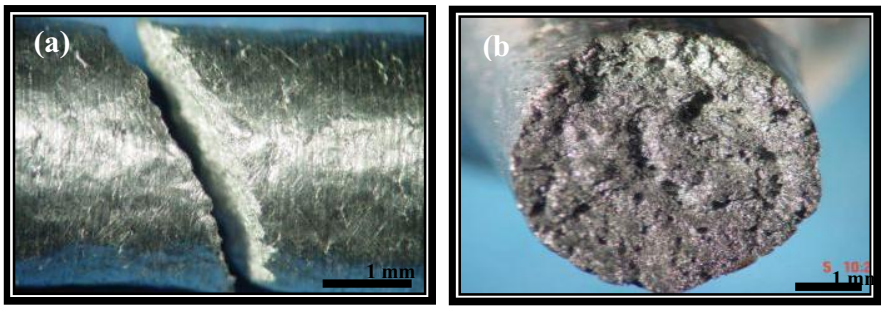

Figure 11. Typical macrographs of tensile fracture surface of cast *in-situ* Al(Mg,Mn)-Al_2O_3(MnO_2) composite cooled after casting in water, containing 2.9 wt% reinforcing particles and 2.4 vol% porosity showing ultimate tensile stress of 239 MPa and percentage elongation of 21.3%.

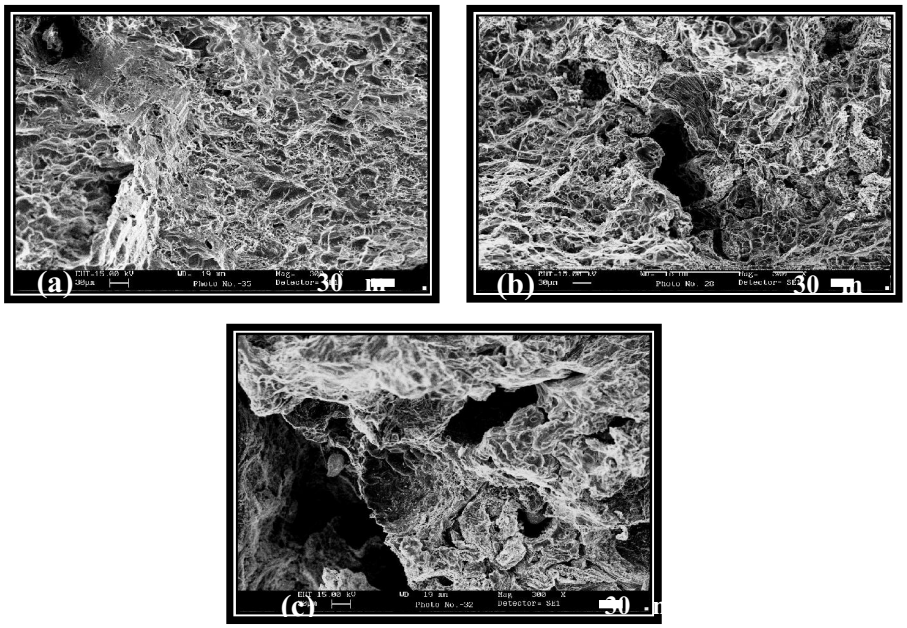

Figure 12 SEM fractographs showing tensile fracture surfaces of the cast *in-situ* composites of nominal composition of Al(5%Mg)-3%MnO_2, synthesized at processing temperature of 730 ^oC for three minutes of processing, followed by different methods of cooling; (a) water cooling; showing ultimate tensile stress of 239 MPa and percentage elongation of 21.3%, (b) air cooling; showing ultimate tensile stress of 192 MPa and percentage elongation of 12.4% and (c) furnace cooling; showing ultimate tensile stress of 82 MPa and percentage elongation of 3.42%.

The processing parameters play an important role for the control of the macro/microstructure and mechanical properties of cast *in-situ* composites. The microstructure of materials affects the wear behaviour of materials a great deal. Hardness and toughness are greatly

affected by the microstructure, which in turn affects the wear properties. It has been well established that the hardness and the topography of the surface affect the number of asperity contacts and the size of each individual contact, in addition to the resistance against deformation of the surface layer. The toughness of materials is closely related to the propagation of cracks, which also affects the rate of delamination. Several different aspects of the microstructure of metals affect the wear process: grain size, volume fraction, size, and distribution of second phase particles and the texture of the surface layer [18]. The wear and friction of cast *in-situ* composite of nominal composition of Al(5%Mg)-3%MnO_2, synthesized at 730 ^{o}C for a given processing time of three minutes, cooled after casting by different cooling rates have been investigated. Results of typical wear behaviour for different cast *in-situ* composites cooled after casting by immersion in water, in air and inside furnace, are shown in Figs. 13(a), (b) and (c) respectively. It is observed that the cumulative volume loss increases linearly with increasing sliding distance and normal load indicating that Archard's adhesive wear equation proposed originally for single phase material, is being followed [19];

$$V = k\,(L\,S\,/\,H)\ldots\ldots\ldots\ldots\ldots\ldots(1)$$

where ***S*** is the sliding distance, ***L*** is the normal load, ***H*** is the hardness of the soft material and ***k*** is the wear coefficient.

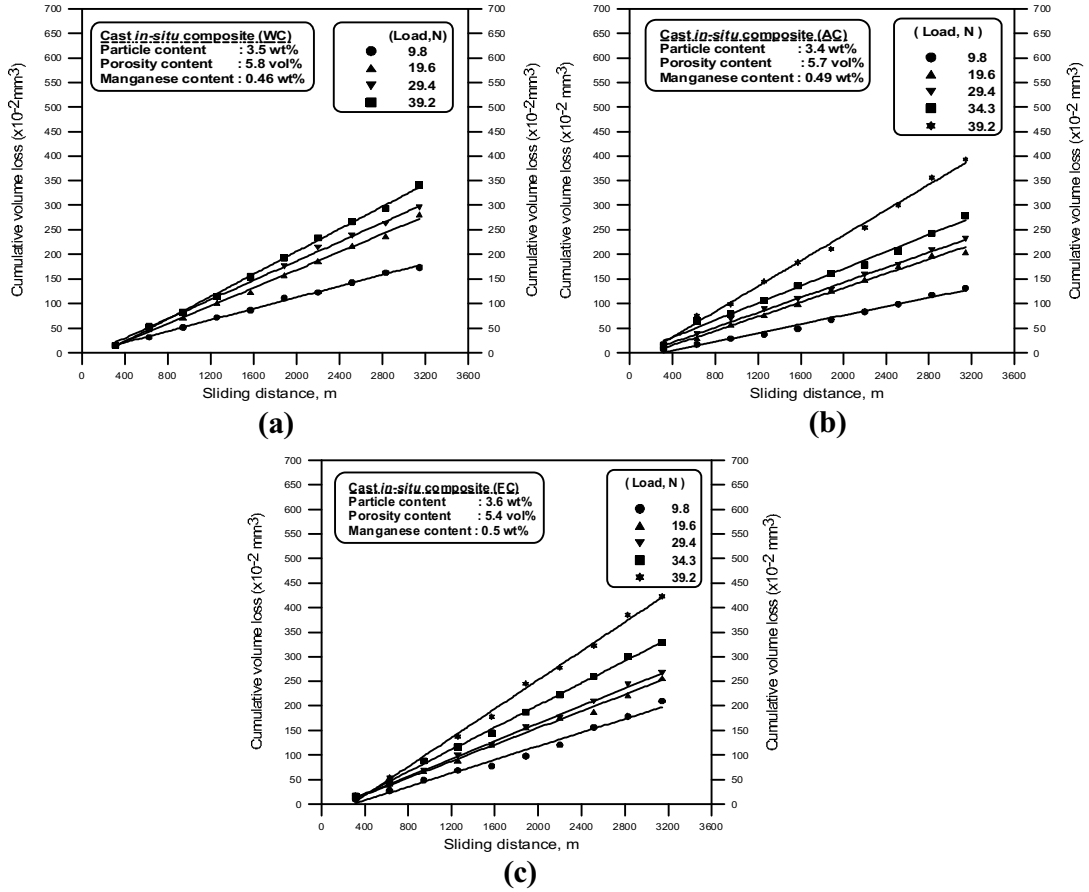

Figure 13. The variation of cumulative volume loss with sliding distance at different normal loads and sliding speed of 1.05 m/s for different cast *in-situ* Al(Mg,Mn)-Al_2O_3(MnO_2) composite cooled after casting by different methods of cooling; (a) water, (b) air and (c) furnace.

It is also observed that the cumulative volume loss, particularly at higher normal load of 39.2 N, in cast *in-situ* Al(Mg,Mn)-$Al_2O_3(MnO_2)$ composite cooled in water after casting, decreases considerably as shown in Fig. 13(a) compared to those observed in the cast *in-situ* composite cooled in air after casting and the composite cooled inside the furnace, as given in Fig. 13(b) and (c) respectively.

The wear rates, ***V/S***, volume loss per unit sliding distance, are determined from the slope of the variation of cumulative volume loss with sliding distance. The wear rate increases more or less linearly with increasing normal load as shown in Fig. 14, for cast *in-situ* Al(Mg,Mn)-$Al_2O_3(MnO_2)$ composites cooled by immersion in water bath, in air or inside furnace after casting. There is considerable decrease in wear rate of cast *in-situ* composite cooled in water after casting, particularly at higher loads, compared to those observed in the cast *in-situ* composites cooled in air or inside furnace after casting. Also, it is observed in Fig. 14 that the difference in wear rate between these three cast *in-situ* composites increases with increasing normal load. Higher hardness due to refined microstructure and superior mechanical properties result in decreased wear rates in cast *in-situ* composites cooled in water after casting in comparison to the wear rates observed in cast ingots cooled in air or inside furnace.

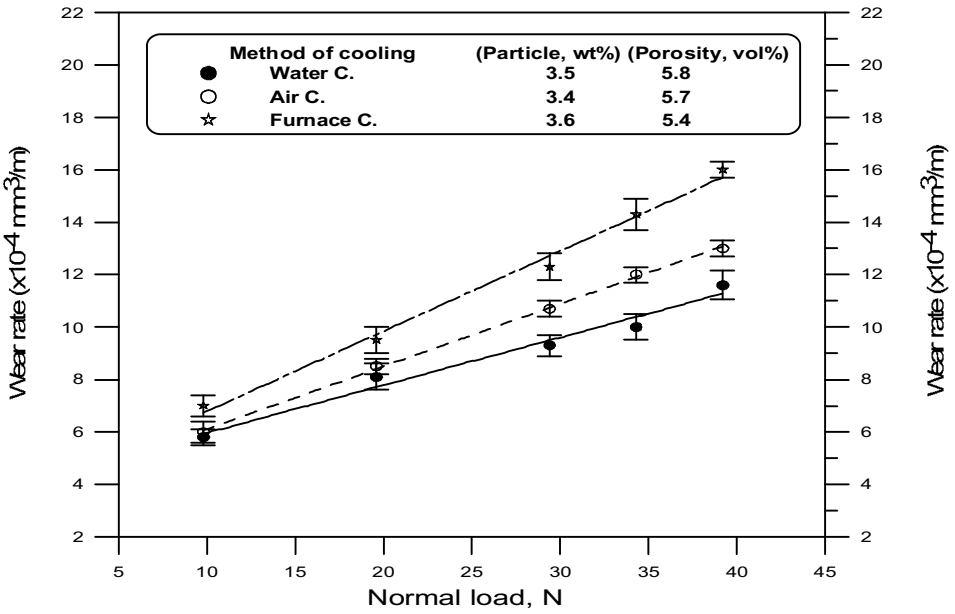

Figure 14. The variation of wear rate with normal load for cast *in-situ* composites of nominal composition of Al(5%Mg)-3%MnO_2, synthesized at processing temperature of 730 ^oC for three minutes of processing time, cooled after casting at different cooling rates.

The typical SEM microphotograph of the worn surface for cast *in-situ* composite cooled after casting by immersion in water bath is shown in Fig. 15. It is observed that the worn surface appears to contain some fine grooves of wear tracks parallel to the sliding direction. Also, some fine oxides in wear debris have got consolidated into transfer layer covering a part of sliding surface. However, there is no significant difference between the worn surfaces for different types of cast *in-situ* composites. Figure 16 shows the typical wear debris for the cast *in-situ* composites cooled after casting by immersion in water bath. The presence of fine oxide particles has been observed in wear debris, as shown in Fig. 16, confirming oxidative wear in the cast *in-situ* composites under the prevailing conditions of test reported here. But there are some metallic

particles as well in the wear debris, sometimes of significantly larger in size, as shown in Fig. 16, which may indicate subsurface cracking and delamination wear as well. In composites containing reinforcing particles and porosity, it is likely that the cracks nucleate at the relatively weaker particle-matrix interface or pores in the deformed layer below the surface, and then propagates to the sliding surface creating particles of wear debris, which is metallic as shown in both Figs. 16.

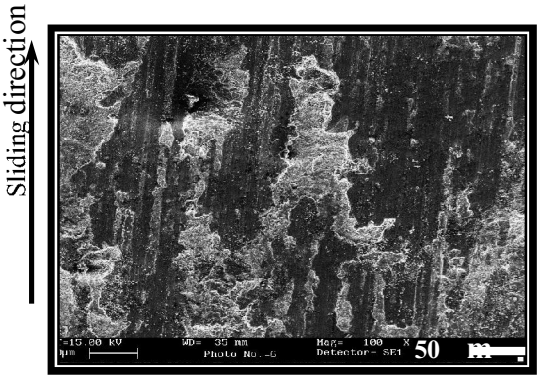

Figure 15. Typical micrograph showing the worn surface of cast *in-situ* Al(Mg,Mn)-$Al_2O_3(MnO_2)$ composite, cooled after casting in water, containing 3.5 wt% reinforcing particle and 5.8 vol% porosity. The normal load is 39.2 N and sliding speed is 1.05 m/s.

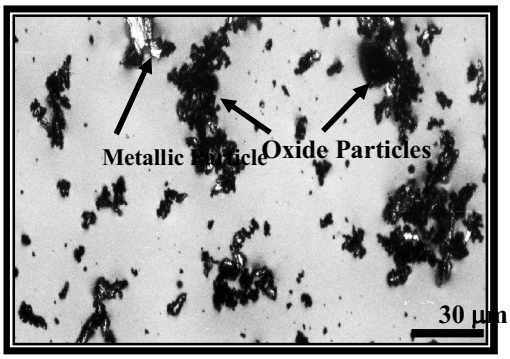

Figure 16. Optical micrograph showing the wear debris of the cast *in-situ* Al(Mg,Mn)-$Al_2O_3(MnO_2)$ composite, cooled after casting in water, containing 3.5 wt% of reinforcing particle and 5.8 vol% porosity resulting from dry sliding against hardened steel disc at sliding speed of 1.05 m/s and normal loads 29.4 N.

The coefficient of friction (μ) is calculated by dividing the recorded frictional force (F) by the normal load (L). Figure 17 shows the typical variation of coefficient of friction with sliding distance for cast *in-situ* composites cooled after casting by different cooling rates, during dry sliding under different normal loads and constant sliding speed of 1.05 m/s. For all the three cast *in-situ* composites, it is observed that at a constant load, the coefficient of friction rises during initial stage of sliding and then fluctuates about a mean value with further sliding. Higher average coefficient of friction is observed in cast *in-situ* composite cooled in water after casting.

Figure 18 shows the typical variation of average value of coefficient of friction with normal load, for cast *in-situ* composites cooled after casting by different cooling rates. For all the three cast *in-situ* composites, it is observed that the coefficient of friction decrease with increasing normal load from 9.8 to 39.2 N. But, it may be noted that in cast *in-situ* composite cooled after casting in water, the rate of decreases is considerably lower than those observed in cast *in-situ* composites cooled after casting in air or inside furnace as demonstrated in Fig. 18. However, this trend of decreasing friction coincides with relatively higher wear coefficient, which could be indicative of change in the mechanism of wear.

The present study clearly reveals the potential of cheap synthesized cast *in-situ* Al(Mg,Mn)-$Al_2O_3(MnO_2)$ composite cooled after casting in water as a candidate tribological material for future engineering applications.

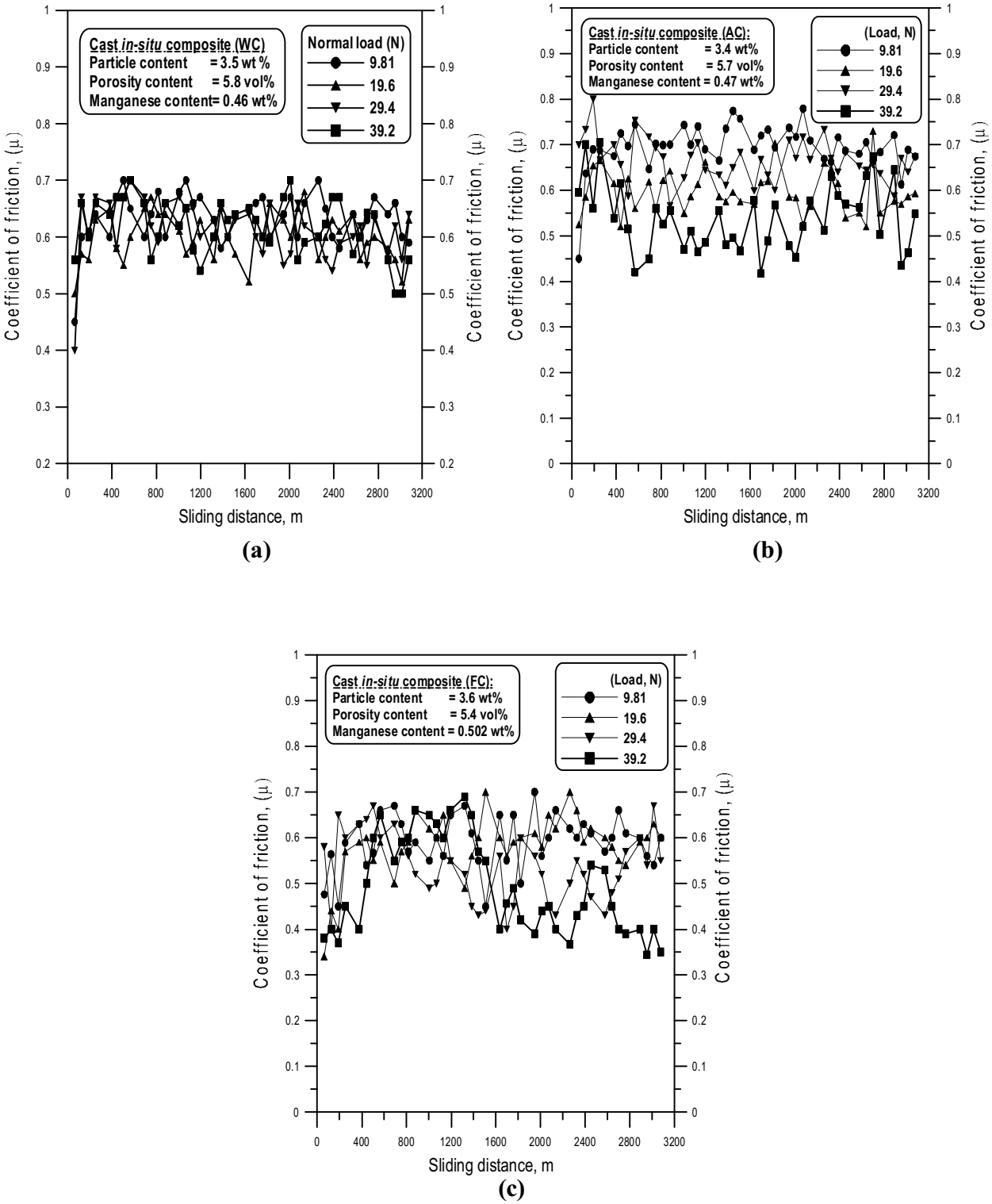

Figure 17. The variation of coefficient of friction with sliding distance at different normal loads and sliding speed of 1.05 m/s for different cast *in-situ* composites of nominal composition of Al(5%Mg)-3%MnO_2, synthesized at processing temperature of 730 ^oC, followed by different methods of cooling; (a) water cooling, (b) air cooling and (c) furnace cooling.

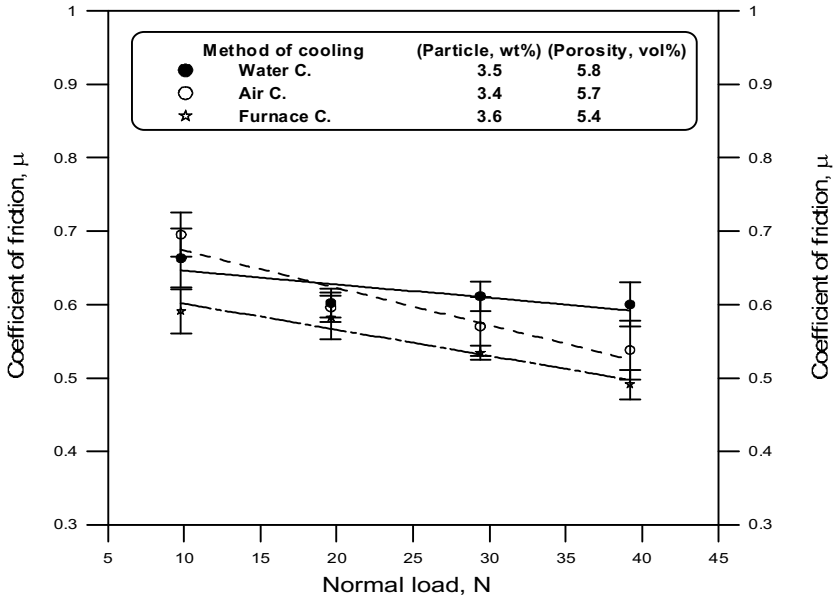

Figure 18. The variation of coefficient of friction with normal load at sliding speed of 1.05 m/s for different cast *in-situ* composites of nominal composition of Al(5%Mg)-3%MnO_2, synthesized at processing temperature of 730 ^{o}C for three minutes of processing, followed by different methods of cooling.

4. Conclusions

In the present study, cast *in-situ* Al(Mg,Mn)-Al_2O_3(MnO_2) composite has been synthesized by dispersion of externally added MnO_2 particles in molten aluminium, followed cooling the cast ingots by different cooling rates. The tribological behaviour of cast *in-situ* composites cooled after casting by different cooling rates, have been investigated. The following main conclusions have emerged.

1. In the cast *in-situ* composites, the size of intermetallic phase $Mn(Al_{1-x}Fe_x)_6$ and the dendrite arm spacing (DAS) increases considerably with decreasing cooling rate of the cast ingot.
2. Higher hardness due to refined microstructure and superior mechanical properties results in decreased wear rate in cast *in-situ* Al(Mg,Mn)-Al_2O_3(MnO_2) composite cooled in water after casting, in comparison to the wear rates observed in cast ingots cooled in air or inside furnace.
3. Superior mechanical properties (tensile properties and hardness) are obtained when the *in-situ* composites are processed by cooling the cast ingot in water after casting as it results in refined microstructure.
4. The cumulative volume loss, particularly at higher normal load of 39.2 N, in cast *in-situ* Al(Mg,Mn)-Al_2O_3(MnO_2) composite cooled in water after casting, decreases considerably compared to those observed in the cast *in-situ* composite cooled in air after casting and the composite cooled inside the furnace.
5. There is considerable decrease in wear rate of cast *in-situ* composite cooled in water after casting, particularly at higher loads, compared to those observed in the cast *in-situ* composites cooled in air or inside furnace after casting. Also, it is observed that the difference in wear rate between these three cast *in-situ* composites increases with increasing normal load. Higher hardness due to refined microstructure and superior

mechanical properties result in decreased wear rates in cast *in-situ* composites cooled in water after casting in comparison to the wear rates observed in cast ingots cooled in air or inside furnace.

6. Cast *in-situ* Al(Mg,Mn)-$Al_2O_3(MnO_2)$ composite cooled in water after casting shows higher coefficient of friction compared to those cooled in air or inside furnace. In refined microstructure the flow of matrix material during sliding may cover the fine intermetallic particles to result in strong junctions of matrix materials with counterface in these areas and increased friction. Coarse intermetallic particles remain exposed and could form weak junctions only and result in relatively lower friction.

References

1. S. Bansal and Subrata Ray, (2005), "Applications of Metal Matrix Composites: A Status Report", 53rd Indian Foundry Congress, 21-23 January, 2005, Kolkata, India, pp. 159-168.
2. S. Ray: J. Mater. Sci., 1993, Vol. 28, pp. 5397-413.
3. R.M. Aikin, Jr.: JOM, 1997, vol. 49, pp. 35-39.
4. J. Goňi, I. Mitxelena, and J. Coleto: Mater. Sci. Tech., 2000, vol. 16, pp. 743-46.
5. Z. Y. Ma, J.H. Li, M. Luo, X.G. Ning, Y.X. Lu, and J. Bi: Scripta Metallurgica-et Materialia, 1994, vol. 31, pp. 635-39.
6. W. Lu, D. Zhang, X. Zhang, and R. Wu: Scripta Mater., 2001, vol. 44, pp. 1069-75.
7. D. Lewis II: "*In-Situ* Reinforcement of Metal Matrix Composites", Metal Matrix Composites: Processing and Interfaces (Treatise on Materials Science and Technology, 1991, vol. 32, Edited by R.J. Arsenault and R.K. Everett, Chapter 6, Academic press, Inc., U.S.A., pp. 121-50.
8. D. Padmavardhani,A.Gomez and R. Abbaschian: Intermetallics, 1998, Vol. 6, PP. 229-32.
9. A.A.Hamid, P.K.Ghosh, S.C.Jain, and S.Ray:Metall. Mater. Trans. A, 2006, vol. 37A, pp. 469-80.
10. P.C. Maity, S.C. Panigrahi and P.N. Chakraborty: Scr. Met. et Mater., 1993, Vol. 28, pp. 549-52.
11. A. A. Hamid, P.K. Ghosh, S.C. Jain, and S. Ray: Metall. Mater. Trans. A, 2005, vol. 36A, pp. 2211-23.
12. K. Geng, W. Lu and D. Zhang: J. Mater. Sci. Letts., 2003, vol. 22, pp. 877-79.
13. A. A. Hamid, P.K. Ghosh, S.C. Jain, and S. Ray: Metall. Mater. Trans. B, 2006, vol. 37B, pp. 519-529.
14. Y.F. Li, C.D. Qin and D.H.L. Ng: J. Mater. Res., 1999, vol. 44, pp. 2997-3000.
15. L. Bangsheng, O. Jiaha, G. Jingjie, Y. Guangjiang, and L. Qingchum: Chinese J. Mater. Res., 1998, vol. 12, pp. 154-58.
16. A. Hiroshi, H. Mitsuji, M. Katsuhisa, S.Yasuhiro, and H.Koji: International SAMPE Metals and Metals Processing Conference, 1992, vol.3, SAMPE, Covina, CA, USA, pp. 581-87.
17. L.F. Mondolfo: "Aluminium Alloys; Structure and Properties", London, Butter worth, 1976, pp. 329-30.
18. N. P. Suh, (1986),"Tribophysics", Prentice-Hall, Inc., A Division of Simon and Schuster Englewood Cliffs, New Jersey, USA, pp.
19. J. F. Archard: "Wear Theory and Mechanism", Wear Control Handbook, Edited by M. B. Peterson and W. O. Winer, ASME, NY, 1980, pp. 35-79.

تم اجراء البحث فى كلية الهندسة – جامعة الموصل